ISSN: 0067-2904

FTIR Analysis and Characterizations of (SnO_2:Ga_2O_3, CeO_2 /Cu_2S/c-pSi) Heterojunctions Solar Cells

Maab A. Abood*, Bushra A. Hasan
Department of physics, collage of science, university of Baghdad, Baghdad, Iraq

Received: 9/4/2022 Accepted: 5/9/2022 Published: 30/5/2023

Abstract

Compounds from tin oxide doped with gallium oxide and cerium oxide were synthesized. Thin films from (SnO_2:Ga_2O_3,CeO_2) with different doping ratios were prepared on glass and single crystal silicon as substrates with the use of the pulsed laser deposition technique. The results of FTIR spectrums analysis was presented. Varies heterojunctions were fabricated from (SnO_2:Ga_2O_3,CeO_2 /Cu_2S/c-pSi) heterojunctions solar cell which are formed from two layers: the first was Cu_2S and the second was layer from tin oxide doped with two oxides named gallium oxide and cerium oxide with different doping ratios (0, 0.03, 0.05, and 0.07). The heterojuntion (SnO_2:5%Ga_2O_3 /Cu_2S/c-pSi photovoltaic structure exhibits open circuit voltage (V_{oc}) of 150mV, short circuit current (I_{sc}) of 15mA, fill factor of 0.622and efficiency of conversion of 2.8% under an intensity of illumination of 100mW/cm^2.

Keywords: solar cell, pulsed laser deposition, SnO_2 thin films, FTIR spectrum

وخصائص المفارق الهجينة للخلايا الشمسيه FTIR تحليل –(SnO_2:Ga_2O_3,CeO_2 /Cu_2S/c-pSi)

مآب عبدالسلام عبود*, بشرى عباس حسن
قسم الفيزياء, كلية العلوم, جامعة بغداد, بغداد, العراق

الخلاصه:

حضرت مركبات من أوكسيد القصدير المطعم بأوكسيد الغاليوم وأكسيد السيريوم. ثم تم تحضير أغشية رقيقة من SnO_2: Ga_2O_3, CeO_2 بنسب تطعيم مختلفة على الزجاج والسيليكون أحادي البلورة كركائز باستخدام تقنية الترسيب بالليزر النبضي ، وتم عرض نتائج لتحليل أطياف FTIR. تم تحضير مفارق هجينة غير متجانسة من (SnO_2: Ga_2O_3, CeO_2 Cu_2S / c–pSi) كخلية شمسية غير متجانسة تتكون من طبقتين الأولى كانت Cu_2S بينما كانت الطبقة الثانية عبارة عن طبقة من أكسيد القصدير مطعم بأكاسيد اثنين هما أوكسيد الغاليوم وأوكسيد السيريوم بنسب مختلفة(0, 0.03, 0.05, 0.07).افضل كفاءة تحويل 2.8%تم الحصول عليها من المفرق (SnO_2:5%Ga_2O_3 /Cu_2S/c–pSi) حيث كانت فولتية الدائرة المفتوحة 150mV وتيار الدائرة القصيرة 15 mA , عامل المليء 0.622, تحت شدة الإضاءة 100mW/cm^2.

*Email: returne.salam@gmail.com

1.Introduction

Nanomaterials were studied in various fields of study, including chemistry, medicine, physics, materials sciences, biology, and pharmacy, due to their unique electronic and optical properties [1,2] . Particles characteristics are improved as their size is reduced. The major strength of nanomaterials to be used in different applications is determined by their chemical and physical features [3]. Cellulose, cerium, titanium, silver, aluminium, iron, tantalum, manganese, gold, or a combination of two or more of these nanoparticles (NPs) are a few of the NPs now being investigated. In addition, Tin oxide can be defined as a semiconducting metal oxide with an n-type band gap of 3.6 eV. It has many applications in solar energy conversion, gas sensing, transparent conducting electrode preparation, catalysis, antistatic coatings, and many more [4].

The existence of impurities and the stoichiometry of SnO_2 in terms of oxygen influences its optoelectronic capabilities. Ga_2O_3 can be defined as one of the significant semiconducting materials [5], and it comes in a variety of crystalline forms known as ε, δ, γ, β, and α phases. It has a 4.9 eV band gap [6]. Due to its surface area/volume ratio, nano-size Ga_2O_3 has unique conduction and semi-conductor characteristics that suggest applications in the opto-electronic devices like photoelectric converters, flat panel displays, and optical limiters for ultra-violet oxide [7]. As a result of solar-blind qualities in a deep UV environment, it could also be employed for fabricating solar-blind devices [8]. Due to its high oxygen ion conductivity, cerium oxide or ceria (CeO_2) has a broad range of applications in oxygen ion conductors in solid oxide fuel cells and catalysts/catalyst supports [9].

2.Experimental

The crystal structure and crystallinity of the tin oxide undoped and doped with Ga_2O_3 and CeO_2 thin films were determined (FTIR 8400s). The spectra of SnO_2 and SnO_2:Ga_2O_3, CeO_2 thin films were recorded in the wavelength range (400-4000)nm.
The Heterojunction solar cells were fabricated , Cu_2S was deposited to increase cell efficiency, a thin layer (SnO_2:Ga_2O_3,CeO_2)was deposited using pulsed laser deposition method on single crystal silicon p-type.

(SnO_2) undoped and doped with different ratios of Ga_2O_3 and CeO_2 compounds and thin films were prepared using pulsed laser deposition method on various substrates like glass, for the FTIR analysis, and single crystal silicon wafers c-Si (p–types). The Si single crystal wafers p-type substrates with crystal orientation of (100), with electrical resistivity in the range of (1.50-5Ω.cm), carriers concentration of $1.45x10^{10}cm^{-3}$, minimal indirect energy gap of 1.10eV were cleaned with the use of the etching process that can be summarized as:
1- Immersing the silicon wafers ,with stirring, in a chemical solution that consists of 3ml HNO_3 and 1ml HF for (1min–3min).
2- Rinsing the samples several times with distilled water.
3- Drying the samples with a soft paper.

The starting materials tin, gallium and cerium oxides were supplied from Alderch company. SnO_2:Ga_2O_3,CeO_2 compounds with different doping ratios (0.0, 0.03, 0.05, and 0.07) were prepared by heating the amounts of matrix oxide with the dopant oxide according to the demand ratios at temperature of 1273 K for five hours, then they were left to slowly cool to the temperature of the room.

Figure 1 shows the structure of the prepared heterojunctions solar cell in the present work. Device structure consists of (from the bottom) a layer of aluminium as back contact

(approximately 200nm), single crystal wafers (p-type silicon) and Cu_2S layer (t=300±10 nm), and finally a layer of SnO_2:Ga_2O_3,CeO_2 of 150nm thickness which was deposited using the pulsed laser deposition method. The top and the bottom contacts were made of silver paste. Current-voltage measurements in the dark were carried out for SnO_2:Ga_2O_3,CeO_2 /p-Si hetrojunctions with Keithley digital electro-meter(616) and a DC power supply. Reverse and forward bias voltages were varied in the range (0V and 1V). I-V illumination measurements were made for the prepared cells by exposure to Halogen lamp light -Philips-120 W and 100mW/cm^2 intensity. The sun-light incident on the device from top as can be seen from Figure 1.

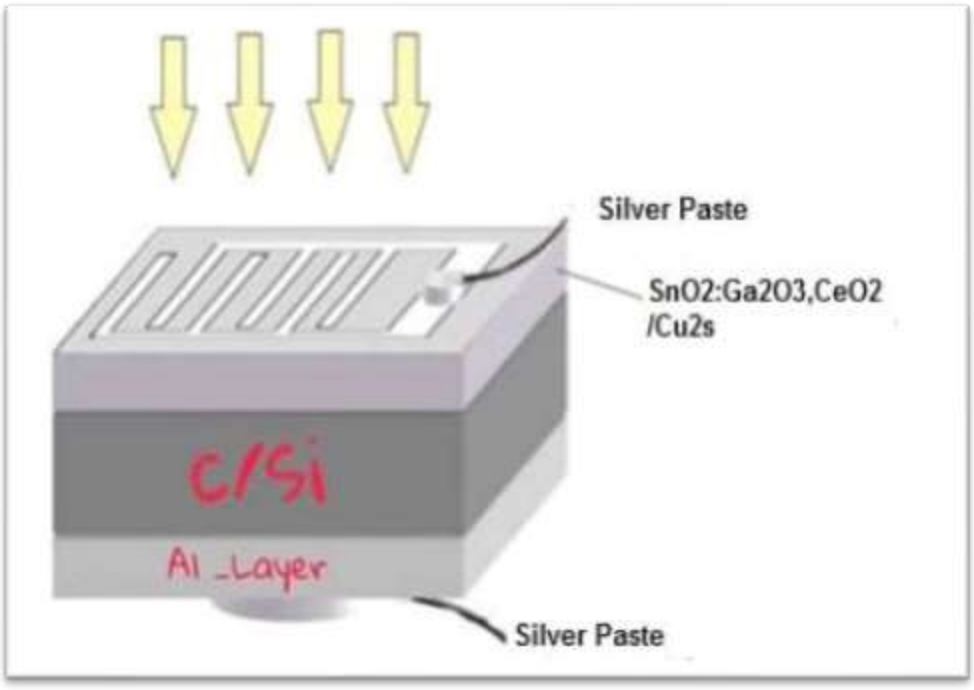

Figure 1: structure of SnO_2:Ga_2O_3,CeO_2 /p-Si solar cell.

From the plots of the relation between bias voltage and forward current, the factor of the ideality (β) could be specified as follows:

$$I = I_o \exp\frac{qV}{\beta k_B T} \tag{1}$$

And the equation of Fill factor (FF)is given by:

$$FF = \frac{V_m I_m}{V_{oc} I_{oc}} \text{ ----------} \tag{2}$$

The photo-voltaic conversion efficiency (PCE) can be characterized as:

$$PCE = \frac{P_m}{P_{in}} = \frac{FFxI_{sc}xV_{oc}}{P_{in}} x100\% \text{ ----------} \tag{3}$$

The value of I_s exponentially decreases with Eg based on the relation:

$$I_S = AqN_c N_v (\frac{1}{N_A}\sqrt{\frac{D_n}{\tau_n}} + \frac{1}{N_D}\sqrt{\frac{D_p}{\tau_p}}) \exp(\frac{-E_g}{kT}) \tag{4}$$

and V_{oc} is associated with the saturation current based on the relation:

$$V_{OC} \approx \frac{kT}{q} \ln\frac{I_L}{I_S} \tag{5}$$

The I-V Characteristics can be described as follows [10]:

$$I = I_{01}[\exp[\frac{qV}{\beta_1 kT}] - 1] + [I_{02}[\exp[\frac{qV}{\beta_2 kT}] - 1] + \frac{q(V - IR_s)}{R_{sh}} \quad (6)$$

Where: I represents reverse saturation current, V represents applied voltage, q represents electronic charge, T represents temperature, k represents Boltzmann's constant, β represents factor of ideality, R_s and R_{sh} are series and shunt resistance values, respectively.
The structures of the (SnO_2):(Ga_2O_3,CeO_2) thin films with different doping ratios were examined using X-ray diffraction. The results showed that all the prepared thin films have polycrystalline structure with tetragonal phase with preferred plane of crystal growth along (110) where the crystal size get to grow from 40.3 nm to 64.5 nm and to 43.5 nm for Ga_2O_3 and CeO_2 doped tin oxide thin films, respectively [11].

3.Results and discussion

3-1 Structural analyses of (SnO_2):(Ga_2O_3,CeO_2) thin films

The FTIR spectra of SnO_2 and (SnO_2:Ga_2O_3, CeO_2) thin films were measured in the range of 400-4000 cm^{-1} for Pure SnO_2. The specific peaks were identified and matched with the standard values done by previous researches. Figure 2 shows the FTIR spectra for pure SnO_2 thin films. The bands were assigned due to the absorption peaks of Sn–O, Sn–O–Sn, Sn–OH and C–O, bond vibrations. In which the strong absorption band at 3416.34 cm^{-1} and the band at 1514.12 cm^{-1} are due to the existence of OH on the adsorbed water and Sn–OH. A sharp peak appeared at 2378.23 cm^{-1} due to carbon dioxide, which is incorporated from the atmospheric exposure. The absorption peak at 663.51 cm^{-1} is assigned to Sn–O vibrations of SnO_2.

The FTIR spectra of the synthesized Ga_2O_3 doped SnO_2 with doping concentrations of (0.03, 0.05, and 0.07) are shown in Figures (2, 3, and 4). The spectra peaks at 613 and 459 cm^{-1} are assigned to Ga–O–Ga and Ga–O vibration of Ga_2O_3, respectively [12]. It was noted that with the increase of the doping concentration, the infrared absorption becomes stronger indicating that the content of Ga–O–Ga and Ga–O has increased. Figures (5, 6, and 7) show the FTIR spectra of the synthesized CeO_2 doped tin oxide with doping concentrations of (0.03, 0.05, and 0.07). The large broad band at 3419.79 cm^{-1} is ascribed to the O-H stretching vibration in OH^- groups. The absorption peaks around 1643.35 cm^{-1} were assigned to the bending vibration of C-H stretching. The strong band below 655.80 cm^{-1} was assigned to the Ce-O stretching mode [13]. The broad band, corresponding to the Ce-O stretching mode of CeO_2 is seen at 500 cm^{-1}.

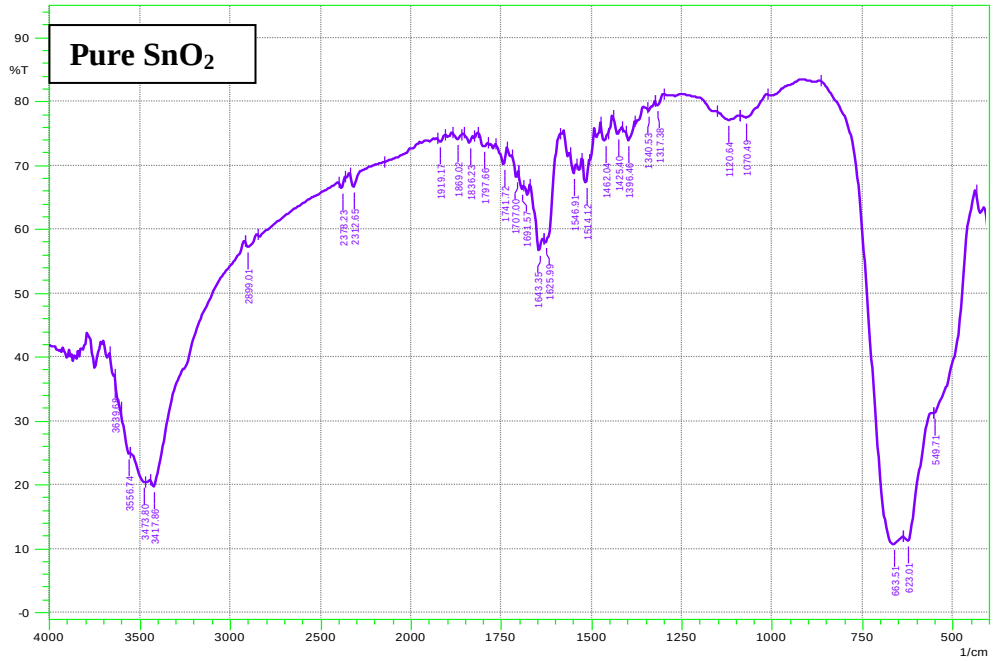

Figure 2: FTIR spectrum of pure SnO_2 thin films

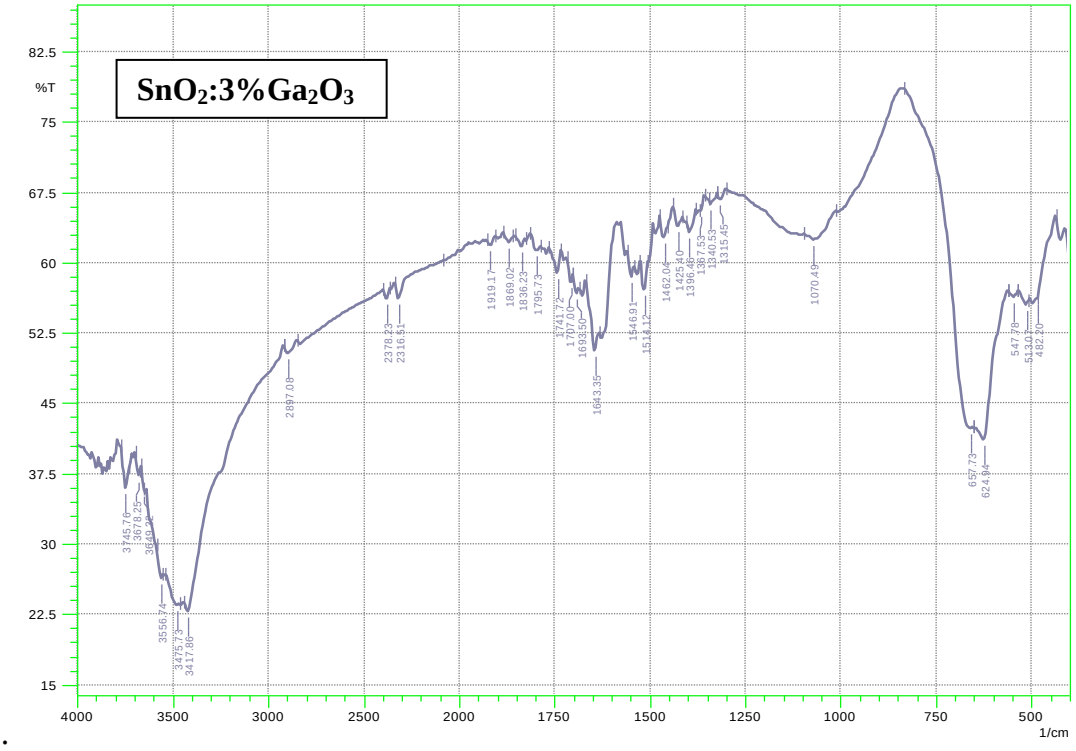

Figure 3: FTIR spectrum of SnO_2:3%Ga_2O_3thin films

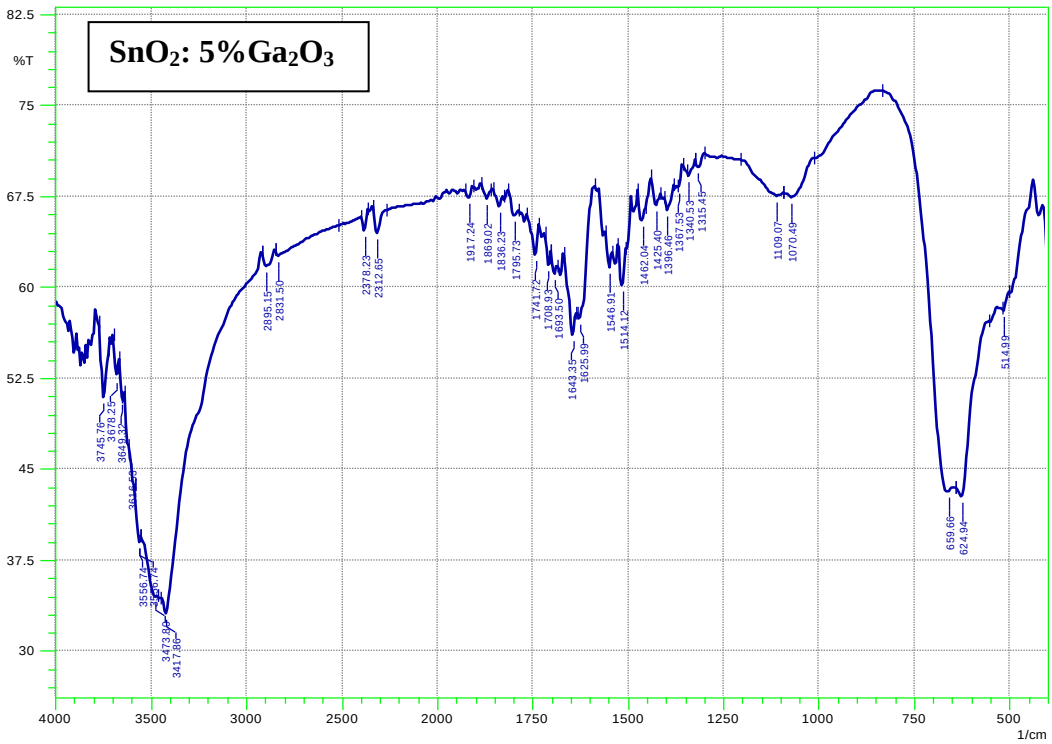

Figure 4: FTIR spectrum of SnO_2:5%Ga_2O_3 thin films

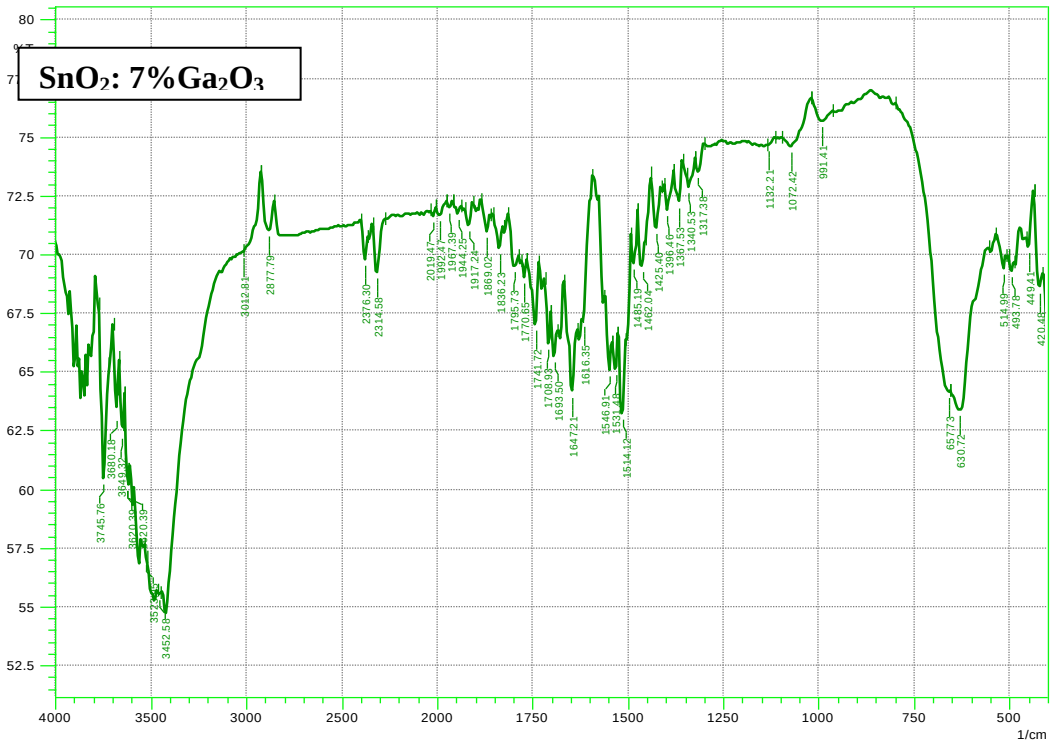

Figure 5: FTIR spectrum of SnO_2:7%Ga_2O_3 thin films

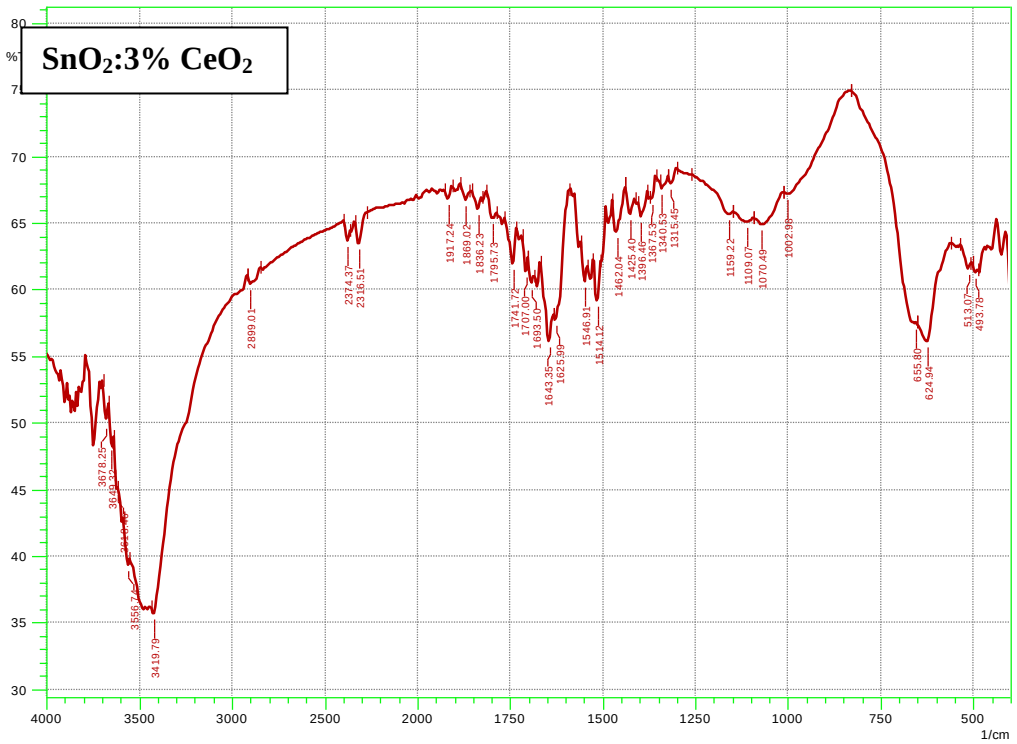

Figure 6: FTIR spectrum of SnO_2:3%CeO_2 thin films

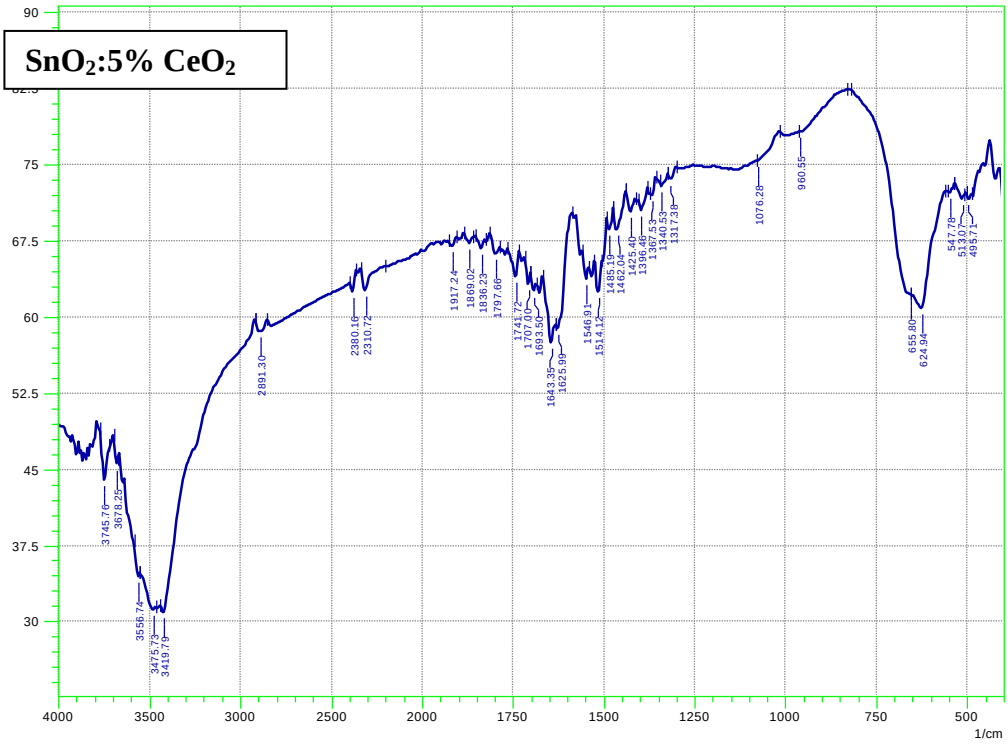

Figure 7: FTIR spectrum of SnO_2:5%CeO_2 thin films

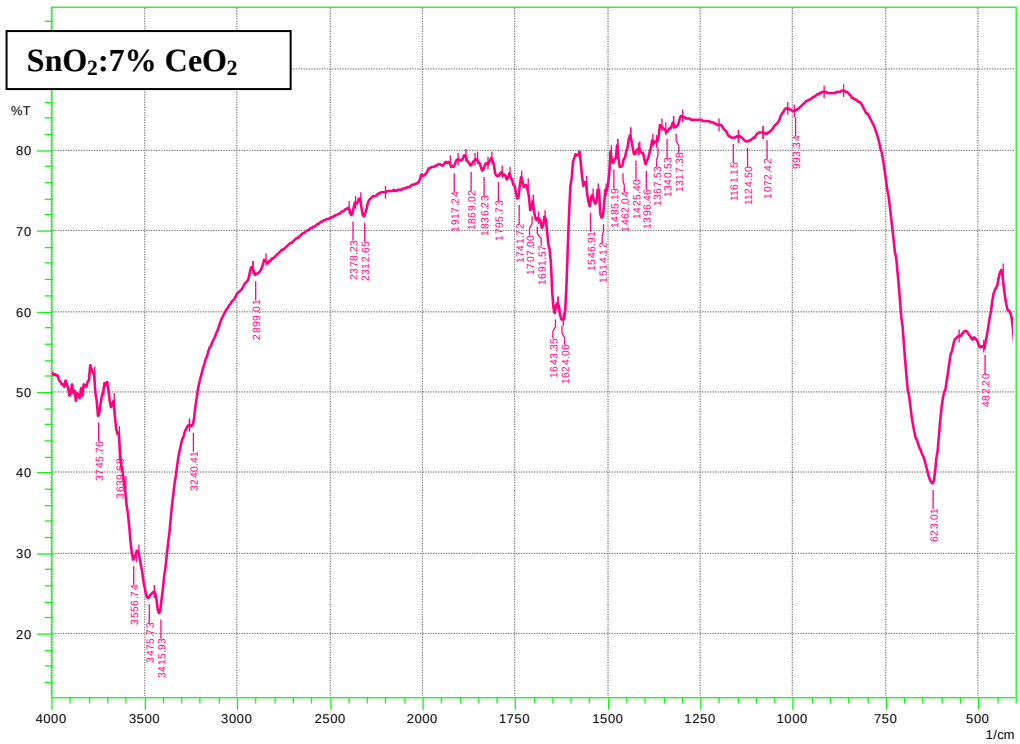

Figure 8: FTIR spectrum of SnO_2:**7%CeO_2** thin films

3.2 Electrical properties

3.2.1 Current –voltage characteristics of (SnO_2:Ga_2O_3,CeO_2 /Cu_2S/c-pSi) heterojunctions solar cells.

In general the forward dark current is generated due to the flow of majority carriers and the applied voltage injects majority carriers which lead to the decrease of the built - in potential, hence decreases the width of depletion layer . One can recognize two regions when forward voltage is applied for all the prepared heterojunctions from (SnO_2:Ga_2O_3,CeO_2 /Cu_2S/c-pSi) as shown in Figure (9a and 9b). The low biasing voltage region where the current is generation recombination here, the generated carriers are greater than the intrinsic carriers i.e. $np>n_i^2$. The high biasing voltage region, the current is attributed to tunneling effect. When reverse bias voltage is applied also two regions can be noted. In the first region of low voltages, where the generation current dominates, the increase of the applied voltage leads to the increase the depletion width, while at the second high voltage region, the diffusion current dominates [14].

In order to estimate the value of ideality factor (n) the relation between forward of (ln dark current) and biasing voltage (0V-0.2V) for (SnO_2:Ga_2O_3,CeO_2 /Cu_2S/c-pSi). respectively were prepared with different gallium and cerium oxides ratios as shown in Figure 10 . It is clear that there are two regions: in the first the recombination current dominated, while the tunneling current dominated at the second region, hence it obeys the recombination-tunneling mechanism. The significant feature of this figure is the non-ohmic behavior, where current flow in the forward biasing, but very low current flows in the reverse biasing.

It is obvious from this figure that the value of the current decreased with increasing the gallium concentration, however the dark current show significant increase with high gallium oxide ratio, i.e . 7%.; while the dark current was low for 3% and 7 % ratios of cerium oxide but significantly increased at 5% ratio. In general, the forward dark current is generated due to

the flow of majority carriers and the applied voltage injects majority carriers which lead to the decrease of the built - in potential, hence decreases the width of depletion layer. The diode ideality factor (β) is an important parameter that determines the quality of the junction, where β approaching unity is considered ideal. According to Sah et al. [15], an ideality factor $0 < \beta \leq 1$ at low voltages and $\beta \rightarrow 2$ at higher voltages were predicted. The range of β, $1 < \beta < 2$ indicates the existence of surface and interface states at junction, which has made it non-ideal for Shockley– Reed–Hall type re-combination. This theory does not address the ideality factor $\beta > 2$; rather than that, a coupled defect level mechanism of re-combination was predicted theoretically [16] and the proven experimentally [17]. These two theories, on the other hand, do not account for the ideality factor $\beta > 6$. It has been suggested by Sze [18] compared to an amorphous or disordered interface layer at junction may cause such a large value of β where Frenkel–Poole (FP) model might adequately describe the conduction properties [18].

According to the structural analysis, increasing the gallium oxide ratio leads to considerable structure enhancement, implying a lower possibility of integrating defects as interface states, which limits charge carrier re-combination [19]. For gallium oxide ratios of 0, 0.05, and 0.07, diode ideality factor β was found to be in an appropriate range, however it quickly increased for 0.03 gallium oxide ratio. Because the obtained factor of ideality β is slightly higher compared to its normal range, $1 < \beta < 2$, it may be assumed that there are defects in both quasi-neutral and junction regions and are accountable for carrier recombination at the junction. It is widely known that the V_{oc}, I_{sc}, and F.F of solar cells must all be improved for enhancing cell efficiency.

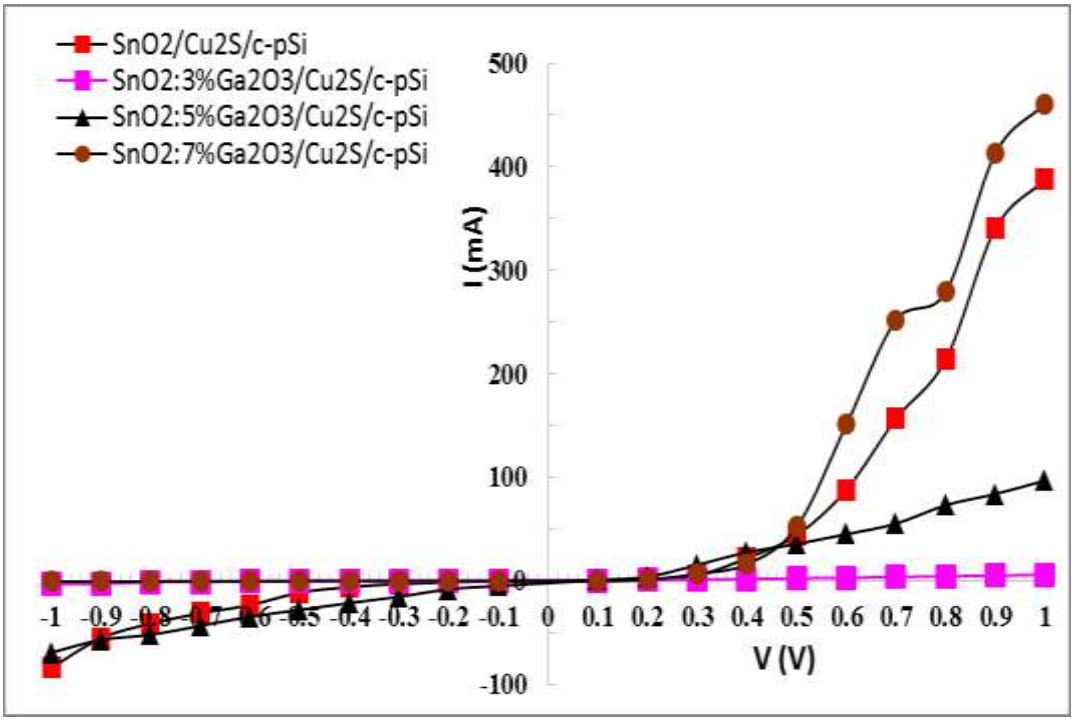

Figure 9a: Current versus applied voltage in dark of (SnO_2: Ga_2O_3 /Cu_2S/c-pSi) heterojunctions.

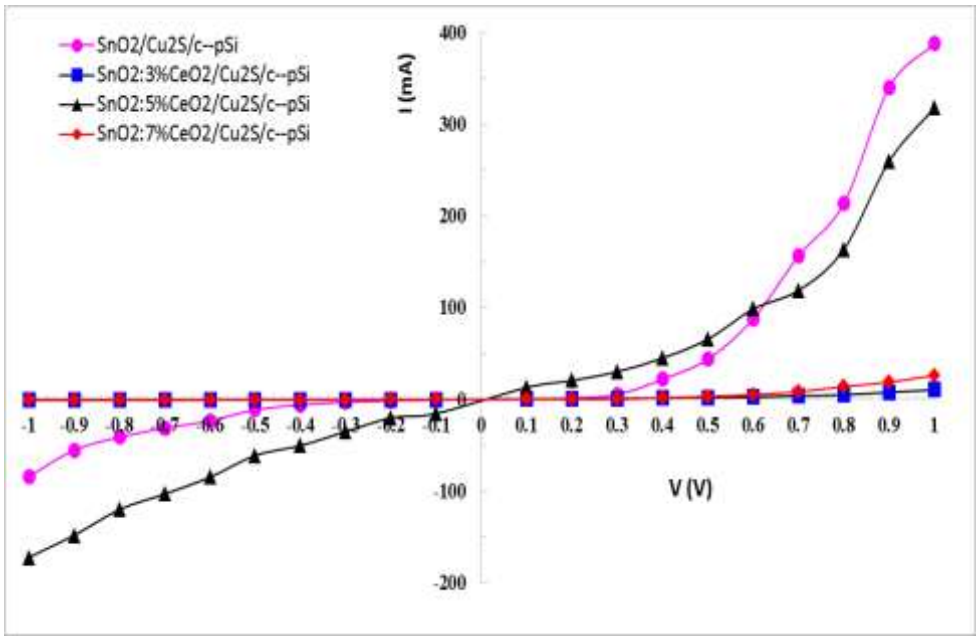

Figure 9b: Current versus applied voltage in dark of (SnO_2: CeO_2 /Cu_2S/c-pSi) heterojunctions.

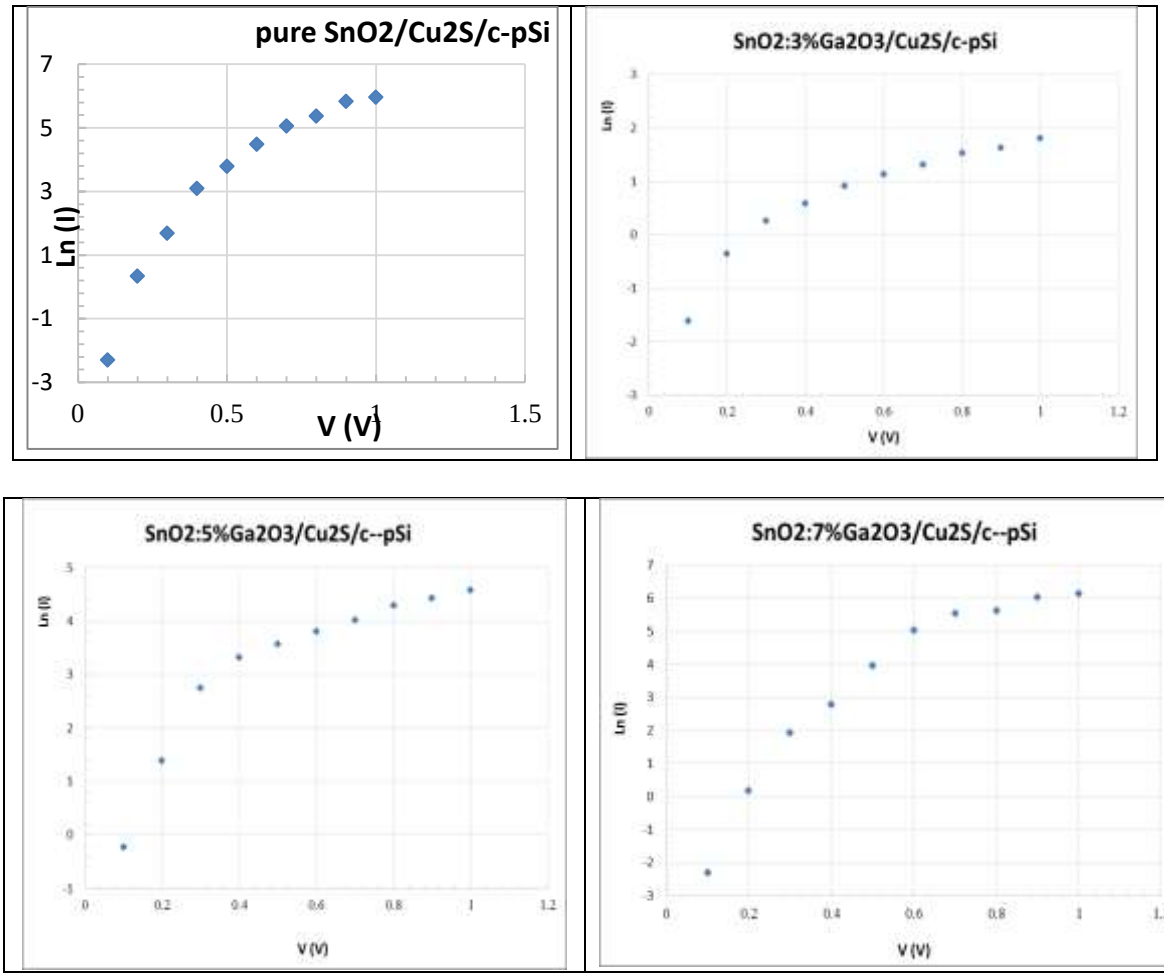

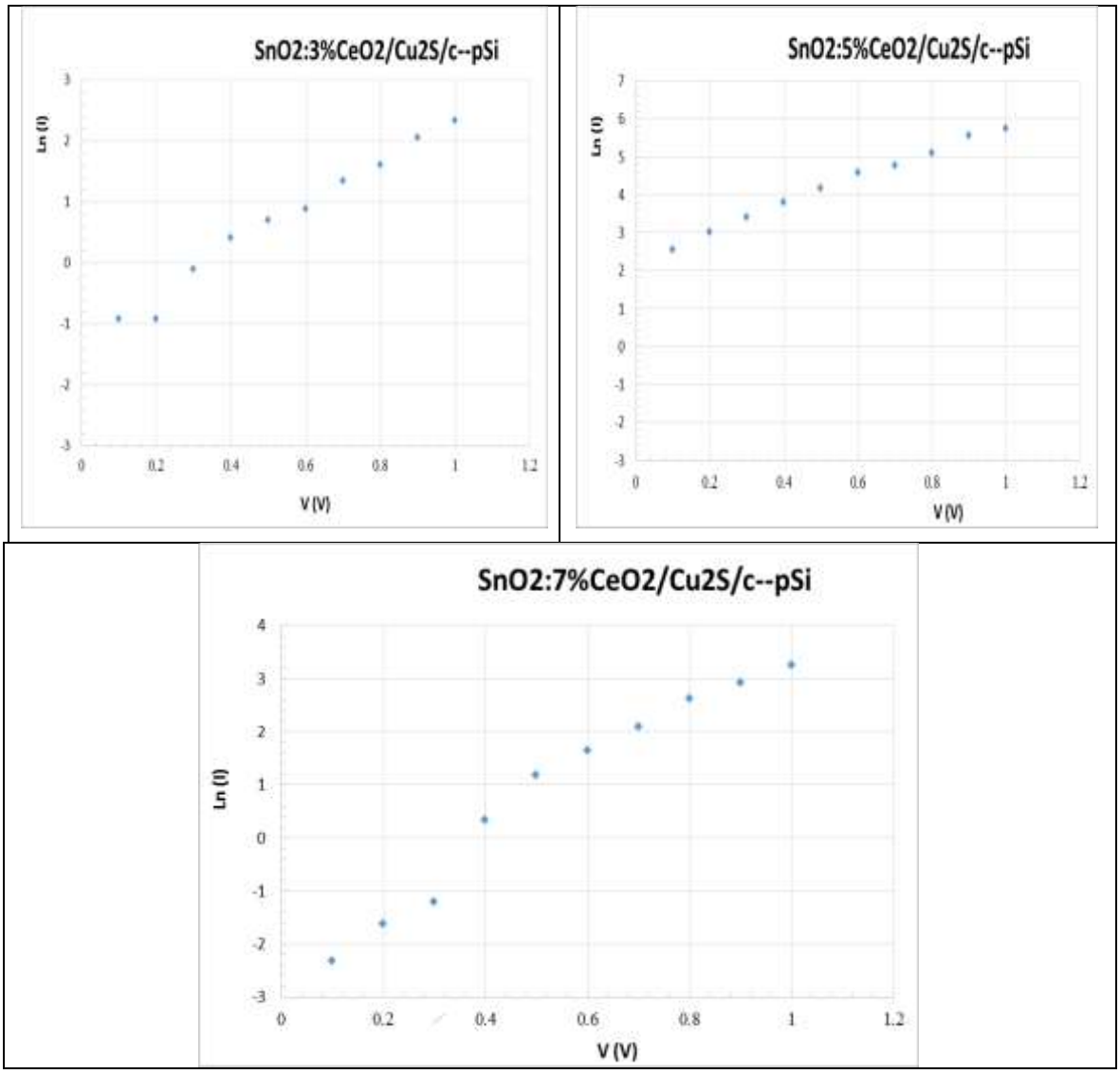

Figure 10: ln(forward current) versus applied voltage of (SnO_2:Ga_2O_3,CeO_2 /Cu_2S/c-pSi) heterojunctions.

Figure 11 shows the current vs applied voltage of (SnO_2:Ga_2O_3,CeO_2/Cu_2S/c-pSi) heterojunctions under standard illumination conditions (100mW/cm^2). Built-in voltage V_{bi} is known to be connected to V_{oc}, with the latter's maximum value being near to the energy gap. The density of charge carriers passing across the junction determines the change in photo current. There is a chance that band-gap discontinuities will form across the absorber layer(Cu_2S), resulting in a reduced V_{oc}. Surface barrier, which has been calculated to be around half of absorber band gap which were (SnO_2:3.60, 3%Ga_2O_3:3.90, 5%Ga_2O_3:2.80, 7%Ga_2O_3:3.50, 3%CeO_2:3.60, 5%CeO_2:3.58, 7%CeO_2:3.55 [11] can also be a source of low V_{oc}. Second, lack of thickness uniformity in absorber layer could result in a significant number of photocurrent shunting paths, producing FF degradation. The diode ideality factor could be greater than 2 as defect density increases. A back contact's series resistance is also an important source of resistance. Silver paste as a back metal contact was employed in the present study, which could result in a high series resistance. Table 1 summarizes the extracted device performance parameters, including open circuit voltage, short circuit current, maximum voltage and current, filling factor, and efficiency. One of the optoelectronic characteristics for heterojunction that is considered a significant parameter which is of high importance in solar cell devices is the current-voltage characteristic under illumination. Figure

10 shows that the photo-current increased as the bias voltage was increased as a result of the narrowing of depletion region, and that the photo-current in reverse bias was greater than that in forward bias. Which is due to the fact that when the applied reverse bias voltage increases, the width of depletion area widens, resulting in separation of electron–hole pairs, and so the photo-current is a function of carrier generation and diffusion. Semiconductors utilized in heterojunction solar cells have a high absorption coefficient when photon energy are much above the band gap energies. This results in significant surface recombination and a drop in quantum efficiency. Reducing the thickness of one junction layer is one approach to reduce this undesired absorption. Yet, this must be accomplished without significantly increasing the device's series resistance, as this would have the opposite effect. As a result of the narrowing of optic band gap and sufficient optical absorption that results, the produced cells have a larger I_{sc}.

On the other hand, it is obvious that SnO_2: 5%Ga_2O_3, PCE (power convertion efficiency) is further boosted by 2.80%. Higher Ga_2O_3-doping (7%) achieved high V_{oc} (0.15V) and fill factor (F.F.=0.667) due to an elevation in the value of the band edge, as seen from the data listed in Table 1. However, this high Ga_2O_3 doping level (7%) results in decreasing $I_{SC,}$ due to the fact that too high a band edge impedes the photo-electrons injection, which thus results in degrading the PCE. It is clearly observed that the conversion efficiency of (SnO_2:Ga_2O_3 /Cu_2S/c-pSi) are higher than those of (SnO_2:CeO_2 /Cu_2S/c-pSi); this may be attributed to the structure enhancement that happened as Ga_2O_3 was added to tin oxide; also the structural analysis showed that the crystal size grew from 40.3 nm to 64.5 nm as a result of doping with Ga_2O_3 ; while, the crystal size increased slightly from 40.3 to 43.5 nm as result of doping with CeO_2 [11]. The high conversion efficiency occurring at 5% Ga_2O_3 doping ratio is related with the lowest energy gap(2.8eV) obtained as a results of doping by Ga_2O_3. It is well known that there is inverse relation between photo current and energy gap [18]. It is well known that built in voltage V_{bi} is associated to V_{oc} and maximal value of the latter is close to the energy gap. The change of photo current depends on the density of charge carries that passes through the junction. The reduction of energy gap suggest reduction of built in voltage, this can be explained as follows.

Large E_g results in large V_{oc} according to equations (4 and 5), and decreasing E_g leads to reducing V_{oc}. The efficiency of the power conversion depends on the efficiency of the absorption, efficiency of exciton dissociation, transportation of the charge carriers and the efficiency of the charge collection. Absorption of the incident photons and the exciton dissociation are decided by photo-active layers' thickness.

The best performance can only be achieved by the optimization of various parameters. It exhibits a semiconductor / semiconductor multijunction thin film behavior with the forward direction to the positive potential on p-S . Such exponential dependence at such range of the voltage may be a result of depletion region formation between n- (SnO_2:Ga_2O_3,CeO_2) active layer and Cu_2S as a result of high work function of the two ohmic contacts for the active layer and (SnO_2:Ga_2O_3,CeO_2).

The relative high conversion efficiency (2.8%) is attributed to high photo current(14mA) provided from SnO_2:5% Ga_2O_3/Cu_2S/c-pSi, while the reduction of photo currents of which are related to wide energy gap of SnO_2: CeO_2 which consequently lead to reduction of conversion efficiency of SnO_2: CeO_2 /Cu_2S/c-pSi cells.

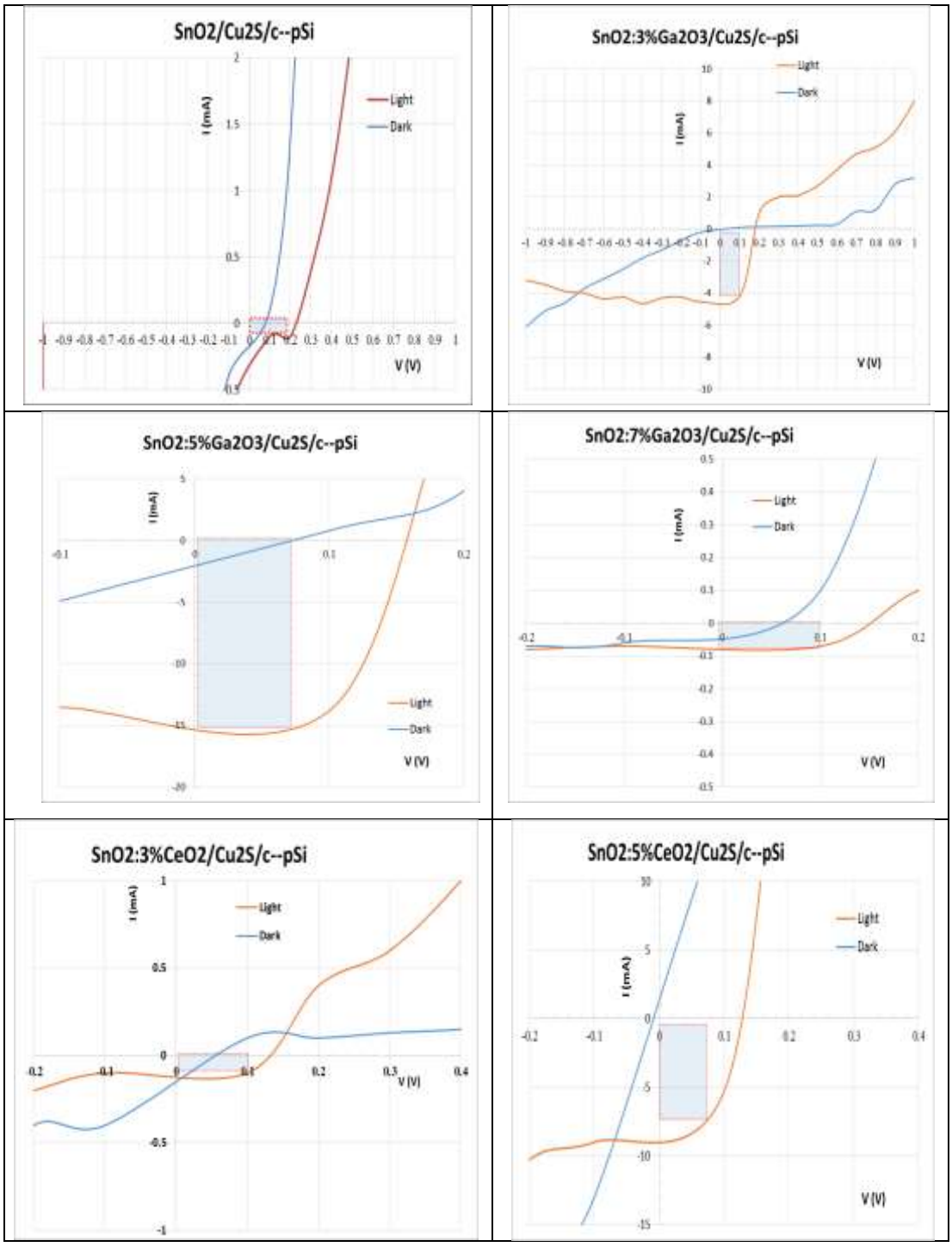
SnO2/Cu2S/c--pSi
I (mA)
V (V)
Light
Dark
SnO2:3%Ga2O3/Cu2S/c--pSi
I (mA)
V (V)
Light
Dark
SnO2:5%Ga2O3/Cu2S/c--pSi
I (mA)
V (V)
Light
Dark
SnO2:7%Ga2O3/Cu2S/c--pSi
I (mA)
V (V)
Light
Dark
SnO2:3%CeO2/Cu2S/c--pSi
I (mA)
V (V)
Light
Dark
SnO2:5%CeO2/Cu2S/c--pSi
I (mA)
V (V)
Light
Dark

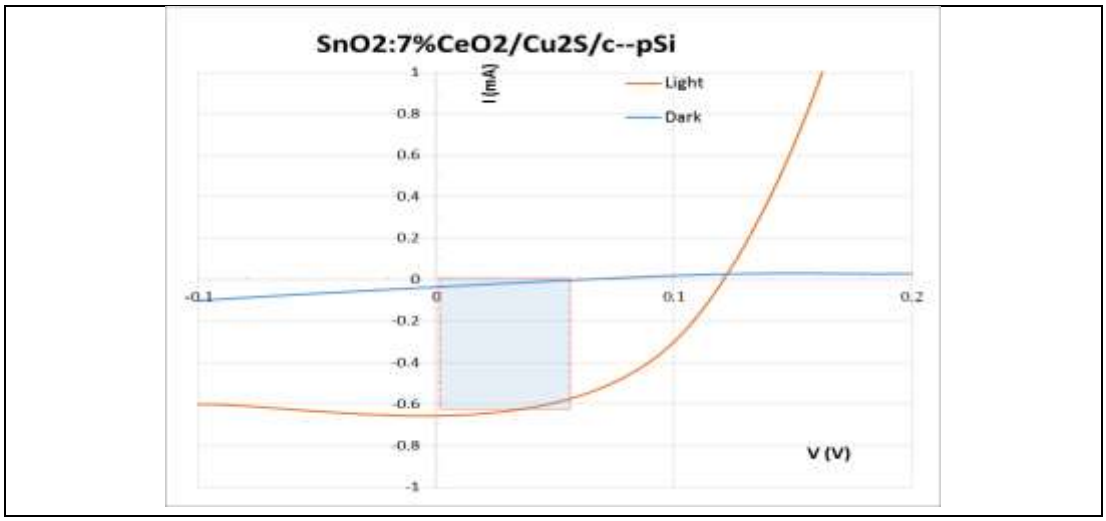

Figure 11: I-V characteristics of (SnO_2:Ga_2O_3,CeO_2 /Cu_2S/c-pSi)

Table 1: The values of I_{sc}, I_m, V_{oc}, V_m, *F.F*, Pm, *Efficiency* and Ideality factor of SnO_2: Ga_2O_3, CeO_2 /Cu_2S/c-pSi heterojunctions solar cells

Sample	I_{sc} (mA)	I_m(mA)	V_{oc}(Volt)	V_m(Volt)	*F.F*	Pm (mW)	*Efficiency*	Idealit y factor
n-SnO_2 /Cu_2S/c-pSi	0.35	0.20	0.22	0.18	0.468	0.036	0.07%	2.01
n- SnO_2:3% Ga_2O_3/Cu_2S/c-pSi	4.50	4.20	0.15	0.20	1.244	0.84	1.68%	12.37
n-SnO_2:5% Ga_2O_3/Cu_2S/c-pSi	15.0	14.0	0.15	0.10	0.622	1.40	2.80%	2.70
n-SnO_2:7% Ga_2O_3/Cu_2S/c-pSi	0.10	0.10	0.15	0.10	0.667	0.01	0.02%	1.90
n-SnO_2:3%CeO_2/Cu_2S/c-pSi	0.10	0.10	0.16	0.13	0.813	0.01	0.03%	10.72
n-SnO_2:5%CeO_2/Cu_2S/c-pSi	9.00	7.00	0.12	0.08	0.519	0.56	1.12%	9.67
p-SnO_2:7%CeO_2/Cu_2S/c-pSi	0.60	0.60	0.10	0.06	0.600	0.04	0.07%	8.73

Conclusions

In the present work, heterojunction solar cells were fabricated from (SnO_2:Ga_2O_3,CeO_2 /Cu_2S/c-pSi).The efficiency depends on whether the doping lead to significant enhancement of the crystal structure or little, since the doping by gallium oxide enhanced the crystal structure compared with doping with cerium oxide, the best efficiency 2.8%was related with minimum energy gap which was obtained at 5% Ga_2O_3. Current versus voltage of the synthesized SnO_2: Ga_2O_3, CeO_2 /Cu_2S/c-pSi heterojunctions solar cells revealed that at low forward bias, recombination dominates, whereas at high forward bias, charge transport through the device dominates. Doping was found to have a considerable impact on device performance. The charge carrier tunneling through large barriers of injection is thought to be the cause of the dark current under reverse bias. The overall efficiency of the device (SnO_2:Ga_2O_3, /Cu_2S/c-pSi) was higher than that of the (SnO_2:CeO_2 /Cu_2S/c-pSi). The current–voltage relation was used to compute different photovoltaic characteristics under

global solar radiation. The reduced carrier recombination rate, which comes from crystal structure enhancement, is responsible for the increased power conversion efficiency.

References

[1] A. Gazzi, L. Fusco, M. Orecchioni, S. Ferrari, G. Franzoni, J. S.Yan, M. Rieckher, G. Peng, M. A. Lucherelli, I.. A. Vacchi, " other carbon nanomaterials and the immune system: Toward nanoimmunity-by-design," *J. Phys. Mater*, vol. 3, pp. 034009, 2020

[2] A. Younis, D. Chu, S. Li, A. Younis, D. Chu, "Cerium Oxide Nanostructures and Their Applications. In Functionalized Nanomaterials," IntechOpen: London, UK, 2016; Available online, vol. 1(3), pp. 176-189 2021

[3] A. Asati, S. Santra, C. Kaittanis, J. M. Perez, "Surface-Charge-Dependent Cell Localization and Cytotoxicity of Cerium Oxide Nanoparticles," *ACS Nano*, vol.4, pp. 5321–5331, 2010

[4] H. Ogawa, A. Abe, M. Nishikawa and S Hayakawa, " Hall measurement studies and an electrical conduction model of tin oxide ultrafine particle films," *Journal of Applied Physics*, vol. 53, no. 6, p. 4448, 1982

[5] S. Kumar, C. Tessarek, S. Christiansen, " A comparative study of β-Ga2O, nanowires grown on different substrates using CVD technique," *Journal of Alloys & Compounds*, vol. 587, pp.812-818, 2014

[6] P. Chang, Z. Fan, W. Tseng, " β-Ga2O3 nanowires: Synthesis, characterization, and p-channel field-effect transistor," *Applied Physics Letters*, vol. 87, no. 22, p.431, 2005,

[7] L. Gai, H. Jiang, Y.tian, "Low-temperature synthesis of β-Ga_2O_3 nanorods on SBA-15 microparticles by solvothermal method," *Nanotechnology*, vol. 17, no. 23, p. 5858, 2006

[8] A. Yuehua, C. Xulong, Y. Huang, D. Cui, Q. Wang, "Au plasmon enhanced high performanceβ-Ga_2O_3, solar-blind photo-detector," *Progress in Natural Science: Materials International*, vol. 26, no. 1, pp. 65-68, 2016

[9] A. S. Nesaraj, I. A.Raj and R. Pattabiraman, "Synthesis and characterization of LaCoO based cathode and its chemical compatibility with CeO based electrolytes for intermediate temperature solid oxide fuel cell (ITSOFC)," *Ind. J. Chem. Tech*. vol. 14, pp.154-160, 2007 [10] S.Bisws, A. Modal, D. Mukherjee and P. Pramanik, " A Chemical Method for the Deposition of Bismuth Sulfide Thin Films" *J. Electrochem. Soc*. Vol. 133. p. 48, 1986

[10] B. A.Hasan, M. A.Abood," A Comparison study the effect of doping by Ga_2O_3 and CeO_2 On the structural and Optical properties of SnO_2 Thin Films," *Iraqi Journal of Science*, vol. 64, no. 4, unpulished

[11] M. E. Elnaggar, A. G. Hassabo, A. L. Mohamed, " Surface modification of SiO_2 coated ZnO nanoparticles for multifunctional cotton fabrics," *Journal of Colloid & Interface Science*, vol. 498, pp. 413-422, 2017.

[12] K. Reinhardt, H. Winkler, "Cerium mischmetal, cerium alloys, and cerium compounds. In: Ullmann's encyclopedia of industrial chemistry," Weinheim, Germany: Wiley-VCH, vol. 7 pp. 285–30, 2002

[13] S. M. Sze, K. N. Kwok, "*Physics of Semiconductor Devices," published simultaneously in Canada*, vol. 978, pp. 750-4470, 2007

[14] C. Sah, R. Noyce and W. Shockley, " Carrier Generation and Recombination in P-N Junctions and P-N Junction Characteristics," *Proc. IRE*, vol. 45, no. 9, pp.1228–43, 1957.

[15] O. Breitenstein, P. P. Altermatt, K. Ramspeck and A.Schenk , "The origin of ideality factors N > 2 of Shunts and surfaces in the dark I-V curves of Si solar cell," *European Photovoltaic Solar Energy Conference, Dresden, Germany*. vol. 21, pp 625–28, 2006

[16] M. Brotzmann, U. Vetterm and H. Hofsass, "BN/ZnO Heterojuntion diodes with apparently giant ideality factors," *J. Appl. Phys.*, vol. 06, pp. 063704, 2009.

[17] S. Sze "*Physics of Semiconductor Devices", John Wiley and Sons*, vol. 109, pp.76, (1981)

[18] B. A.Hasan, "Photovoltaic Structure Using Thermally Evaporated Tin Sulfide Thin Films " *International Journal of Advanced Research in Engineering and Technology* (IJARET), vol. 5(1), pp. 91-99, 2014

[19] B. A.Hasan, " Structural and Optical Properties of SnS Thin Films" *International journal of advanced scientific and technical research*, vol. 3, Issue 4, May-June 2014